Hindawi
Wireless Communications and Mobile Computing
Volume 2023, Article ID 7146912, 17 pages
https://doi.org/10.1155/2023/7146912

Research Article

Data-Driven Multiobjective Optimization for Massive MIMO and Hyperdensification Empowered 5G Planning under Realistic Network Environment

Seifu G. Zeleke,[1] **Beneyam B. Haile**,[1] **Ephrem T. Bekele**,[1] **Edward Mutafungwa**,[2] **and Jyri Hämäläinen**[2]

[1]*School of Electrical and Computer Engineering, Addis Ababa Institute of Technology, Addis Ababa University, Addis Ababa, Ethiopia*
[2]*Department of Communications and Networking, School of Electrical Engineering, Aalto University, 02150 Espoo, Finland*

Correspondence should be addressed to Seifu G. Zeleke; seifu.girma@aait.edu.et

Received 27 May 2022; Revised 20 December 2022; Accepted 5 January 2023; Published 20 January 2023

Academic Editor: Changqing Luo

To accommodate the increasing data rate demand, the fifth-generation (5G) cellular network came up with new technological advancements including massive multiple-input multiple-output (massive MIMO) and hyperdensification which can significantly boost network capacity. On the other hand, the introduction of these technologies along with their heterogeneity brings a challenge in terms of network operators' need to identify a cost-effective optimal deployment approach which is hardly entertained by the legacy planning and optimization method. Hence, to leverage the core benefits of those technologies in a cost-effective manner, we need a holistic planning framework that takes into account their coverage, capacity and cost impact, and realistic spatiotemporal distribution of users. In this work, we present a data-driven multiobjective optimization planning framework that can be used not only for small cells but also for massive MIMO. The planning framework is illustrated using a 5G planning case study for a service area in Addis Ababa, Ethiopia, considering its realistic network data that is collected from the network management system and different potential identified deployment options. Ray tracing is employed to compute propagation, and users and demands are distributed based on the realistic network data. A two-stage optimization and a joint optimization are applied to identify points that provide optimal network performance. Simulation results reveal that the planning method provides Pareto points for different deployment options that can significantly improve the performance of the existing network while reducing the total network cost.

1. Introduction

According to many studies, mobile network traffic volumes have been growing steadily in the last two decades and will continue to do so in the foreseeable future [1, 2]. This traffic growth is typically driven by increased penetration of mobile computing devices and adoption of bandwidth-intensive use cases (e.g., remote working or learning and high-resolution video consumption). For instance, the GSMA report from 2021 projected that 70% of the global population will have a mobile subscription by the year 2025, with majority of new subscribers being from Asia and sub-Saharan Africa. In other annual studies by the network equipment vendor Ericsson, it was noted that the amount of traffic carried by mobile networks increased 300-fold within a decade from 2011 to 2021 [2]. Similarly, within the same time period, the average traffic per smartphone increased by a factor of 14. These traffic growth trends oblige mobile network operators to continuously expand their network capacity to meet evolving user and service demands.

The fourth-generation (4G) long-term evolution (LTE) networks are generally considered to be the first type of mobile technology standard that was specified from the beginning to cater to this insatiable demand for capacity for mobile broadband services [3, 4]. This resulted in the aggressive rollout of LTE networks by the network operators

targeting full population coverage while also gradually migrating from preceding (pre-4G) mobile technology generations. However, the pace of mobile data traffic growth and new demands from vertical use cases (e.g., connected cars and public safety) necessitated the evolution of the baseline LTE (Release 8) standard from the Third-Generation Partnership Project (3GPP). These became available in subsequent 3GPP releases in the form of LTE-Advanced and LTE-Advanced Pro enhancements which could be applied as upgrades that protect initial LTE investments by operators [5]. However, despite these continued LTE network enhancements, the commercial rollout of new fifth-generation (5G) mobile technologies (specified from 3GPP Release 15) is now on the timelines of most global operators [6]. This is attributed to the fact that 5G not only provides at least an order of magnitude increase in capacity over LTE (and its incremental enhancements) but also is specified from the beginning to have the versatility to cater to the requirements of diverse vertical use cases [7].

As 5G development is essentially use-case-driven, it has necessitated the specification of a 5G new radio (NR) air interface, with flexible numerology and architectures to meet differing requirements in terms of latency, reliability, and so on, and also improved capacity scalability. The latter is primarily enabled by the exploitation of broader spectrum resources available in high bands (particularly frequency range 2 specified by 3GPP) and the increased spectral efficiency through the use of high-order modulation schemes and massive multiple-input multiple-output (MIMO) antenna configurations. Additional capacity gains in 5G networks are derived from enhanced spectrum reuse through the dense deployment of small cell sites to supplement existing microcellular sites. It is indeed noted that the densification approach began with LTE networks' typical site densities of around 10–30 sites/km^2 [8]. However, the higher capacity targets and high-band operations in 5G networks would necessitate ultra- or hyperdensification with site densities even exceeding 150 sites/km^2 in some outdoor urban [9, 10].

However, while the aforementioned mobile technology developments are compelling in terms of meeting evolving user demand, they present significant complexity for network planners due to the diversity of possible technology deployment or upgrade options and the need for cost-effectiveness to maximize the operator's return on investment (ROI). In its fundamental form, detailed mobile network planning involves evaluating the required number, location, and configuration of base stations to cost-effectively meet projected user demand in a given service area. In an era with 5G expected to dominate new base station deployments or site upgrades, it is essential for the network planning process to respond to operator planning questions, such as the following:

(i) Where are new 5G sites deployed or 5G upgrades implemented on existing LTE sites

(ii) In given high traffic demand areas, should capacity need to be met by dense small cell deployment or should macrocell be upgraded with massive MIMO antennas of a given order

(iii) With virtualised and disaggregated 5G base stations, which 3GPP functional splits for each base station should the functions be placed in the radio access network (RAN)

(iv) How are costs minimized by leveraging candidate sites with existing facilities for backhaul/fronthaul and powering

In a previous study [11], the authors addressed some of these challenges by proposing a holistic network planning framework for hyperdense 5G deployments. The planning framework was characterised as data-driven due to the use of contextual datasets (e.g., network traffic data and morphological data) as input to the planning algorithms. Furthermore, the network planning problem in the framework required multiobjective optimization approaches as it involved simultaneous optimization of conflicting objectives (maximizing performance versus minimizing cost) and had high cardinality (due to the high density of small cells). A Pareto optimal solution of the multiobjective optimization problem is said to be found if it is not possible to improve any objective without degrading at least one other objective.

A notable gap in the study of [11] was the assumption of network hyperdensification with 5G small cells being the only upgrade option considered for scaling capacity in an incumbent 4G macrocellular network. This particular assumption limited the planning scope by not considering other capacity enhancement approaches, for instance, massive MIMO (one of the key enablers of 5G mobile networks) or a combination of the technologies (small cells and massive MIMO). These deployment options may in parts of a service area have an advantage (from a cost or performance perspective) over dense small cells. The discourse on the benefits or trade-offs between 5G massive MIMO versus small cell deployments is well documented in industry and scientific literatures (see, for example, [12]).

This article addresses the aforementioned issues by proposing an extension to the previously proposed data-driven multiobjective optimization framework for 5G network planning by considering not only network densification (with 5G small cells) as the sole upgrade option but also upgrade of macrocellular sites with 5G base stations with massive MIMO antenna configurations as an alternative or complementary solution. The new extended planning framework proposed in this article is validated using a realistic planning case study and reveals the following useful insights when compared to previous or existing approaches:

(i) Upgrading a network with optimized massive MIMO will provide up to 290.5% user satisfaction gain at 10 Pareto massive MIMO networks relative to macro-only configuration with a planning approach that considers user satisfaction as a performance target

(ii) For the case of two-stage joint optimization, it provides up to 664% user satisfaction gain for a combination of 8 massive MIMO and 50 small cell Pareto networks relative to macro-only configuration with a planning approach that considers user satisfaction as a performance target

The rest of the paper is organised as follows. Section 2 presents related work and the identified research gaps. Section 3 discusses the system model that applied the work. In subsections of this section, multiobjective problem formulations, deployment options, and planning approaches are described. Section 4 presents simulation parameters, assumptions, results, and discussion. Finally, Section 5 provides concluding remarks and potential future works.

2. Related Works

The need for more precise network planning is becoming more critical in 5G network deployments due to the relative increased complexity in terms of base station density (both indoor and outdoor), higher-order massive MIMO antenna configurations, and the use of the 5G new radio (NR) beam-based air interface [13]. These demands on network planning further increased the need to consider a heterogeneous technology environment considering not only the diversity of technology options available in 5G but also codeployment with preceding mobile technology generations.

tCurrently, two network planning approaches have been prevalent particularly in 4G or earlier deployments, namely, planning under consideration of either synthetic or realistic environments or some combination of the two. The key distinction between the two is that the planning environment is on the level of utilization of realistic contextual data as input to the network planning process. This specifically applies to (but is not limited to) the following cases:

(i) *Radio Propagation Modelling*. Propagation modelling provides pathloss maps of a target planning area for given deployment topologies and antenna configurations. To that end, the accuracy and spatial resolution of the pathloss map are useful in optimizing coverage and minimizing interference in network planning. Typically, the pathloss predictions may be obtained using either empirical or deterministic propagation models [14]. The empirical models represent a synthetic approach with low computational effort as they are based on models derived from measurements performed in past study locations and only have minimal geospatial data requirements for the target planning areas. By contrast, deterministic models are a more realistic approach that archives modelling accuracy. However, empirical models present higher computational complexity and the need for detailed three-dimensional (3D) geospatial data of the planning area which may include data on building structures and materials, terrain, foliage, and other scatterers in the area.

(ii) *Distribution of Users and Demand*. The network planning decisions on topology and density are impacted by current and future spatiotemporal traffic distribution in the target planning area. This spatiotemporal traffic distribution is determined by variations in user distributions and their respective service demands (in terms of throughput, latency, etc.). In synthetic approaches, user distributions may be approximated by probability distributions (e.g., Poisson and uniform), whereas service demands are represented by common network-wide targets, such as cell edge throughputs. By contrast, data-driven realistic approaches have more realistic spatiotemporal user and service demand distributions. Moreover, the definition of service demands is increasingly being done specifically to each user depending on data on requirements of actual service used or assigned network slice [15].

So far in literature, many network planning and performance analysis studies involving massive MIMO and dense 5G network deployments have been carried out using either realistic or synthetic environments. References [16–18] investigate the performance impact of massive MIMO under synthetic environments. However, as noted previously, these theoretical works do not render the real impact of a realistic network environment, propagation model, user distribution, and network layout.

References [19–23] analyse the performance impact of massive MIMO under realistic environments. The authors in [19] investigate how massive MIMO performs in channels measured in real propagation environments with a 2.6 GHz operating band. Based on measurement data, they illustrate the channel behaviour of massive MIMO and evaluate the corresponding performance. Reference [20] investigates variations in the spectral efficiency due to changes in the user equipment (UE) and base station (BS) antennas of the massive MIMO network in the downlink scenario. Reference [21] studies a massive MIMO system that performs in real propagation environments, specifically on channel performance of a realistic indoor scenario using large linear and circular antenna arrays. In Reference [22], realistic massive MIMO channels are evaluated both in single and multicell environments. The authors in [23] evaluate the user rate performance of massive MIMO small cells in hotspot areas with the use of the 28 GHz millimetre wave band. However, these works do not show how, when, and where to deploy the technology.

Reference [24] provides a model which can be used as guidance for modelling cognitive radio networks (Internet of Things, fifth generation, and cell phone networks) and security performance evaluation. The authors in [25] optimize the capacity of a two-tier network by selecting a set of cochannel users and allocating power among them with a millimetre wave. However, both manuscripts do not address the planning aspect of mobile networks. References [26–38] conducted a planning work with a combination of realistic and synthetic environments. However, they are not data-driven based and do not consider massive MIMO.

References [39, 40] optimize massive MIMO BS locations under Electromagnetic Field (EMF) and power consumption constraints. Reference [39] addresses EMF-aware 5G network planning and, in particular, the problem of site selection for 5G BS equipment that abides by downlink EMF limits. The work considers EMF-aware mobile networking and overviews the current exposure limits and how the EMF constraints may impact 5G planning. Reference [40] proposes a novel method combining hybrid ray tracing-finite difference time domain (FDTD) and network planner tools. Using this method, they proceed with the optimization of the BS's locations under the low power consumption and low EMF exposure constraints. However, both are not data-driven based. Moreover, they do not consider small cells.

References [11, 41] conduct 5G planning works under realistic environments. Reference [41] proposes a method to optimize positions, coverage, and energy consumption of massive MIMO base stations while meeting low power requirements. However, it is neither data-driven based nor considered small cells. Reference [11] proposes a data-driven multiobjective optimization framework for hyper-dense 5G network planning. However, it does not consider massive MIMO. Hence, this work considers a data-driven- and multiobjective optimization-based network planner method for 5G radio access network (RAN) densification with massive MIMO and small cells under a realistic environment. Table 1 acknowledges advances in the literature while also highlighting the gaps.

3. System Model

3.1. Overview of the Planning Framework. As a methodology, this paper adopted the holistic planning framework proposed for hyperdensification in Reference [11]. The approach takes relevant contextual data from the target planning area as an input and provides outputs for Pareto optimal networks. The aim of the evaluation is to help the operator's choice of network deployment.

Massive MIMO incorporated in the proposed framework by manipulating blocks belongs to data collection and data-driven analysis phases so that the multiobjective optimization considers the impacts of the massive MIMO. Pale pink-shaded blocks show the points that need to be incorporated into the extended planning framework (see Figure 1). The framework has three main parts: data collection, data-driven analysis, and multiobjective optimization. Each of them is briefly described as follows.

The data collection part is about achieving accurate relevant planning data including geospatial data for the service area, cost, and revenue-related data. The geospatial data consists of network layout and other geospatial data that affect fading parameters and demand distribution. Data related to existing service areas such as cell configurations, spatiotemporal distribution of users/devices, and their traffic can be obtained from the granular (e.g., hourly) large datasets produced by the operator's network management system (NMS) [42]. The cost and revenue part is associated with the cost of network upgrades, equipment, site acquisition, and fronthaul/backhaul. Data that describes these costs need to be surveyed in the context of the planning area and targets. Total Cost of Ownership (TCO) is a sum of all site deployment costs including location-dependent and location-independent which are given as [11]

$$\begin{aligned} \mathrm{TCO} &= \sum_{j=1}^{N_c} \mathrm{SC}_j + \sum_{j=1}^{N_M} \mathrm{mMC}_j, \\ \mathrm{SC}_j &= \begin{cases} \mathrm{SC}(j, X_c(j) - 1), & X_c(j) \neq 0, \\ 0, & X_c(j) = 0, \end{cases} \\ \mathrm{mMC}_j &= \begin{cases} \mathrm{mM}(j, X_c(j) - 1), & X_c(j) \neq 0, \\ 0, & X_c(j) = 0, \end{cases} \end{aligned} \tag{1}$$

where $\mathrm{SC} \epsilon \mathbf{R}^{N_c x N_o}$ and $\mathrm{mMC} \epsilon \mathbf{R}^{N_M x N_o}$ are the cost of the matrix with values for small cell candidate sites and cost of matrix associated with massive MIMO, respectively. N_c and N_M are described as the number of small cells and massive MIMO candidate sites. In this work, the existing macrosites are considered candidate site locations for massive MIMO.

The data-driven analysis part incorporates geospatial modelling, propagation prediction, user and demand distribution, and selection of candidate sites. In geospatial modelling, topography and building need to be accurately modelled. After geospatial modelling, propagation modelling is done for existing macro-, candidate massive MIMO, and small cells. The resulting average channel power response is given $\gamma = \mathbf{R}^{N_t x N_\alpha}$, where $N_t = N_m + N_M + N_C$, where N_t is the number of existing cells, N_M is the number of massive MIMO candidate sites, N_C is the number of small cell candidate sites, and N_a is the number of area elements (pixels) in the planning area. After propagation computation, users and demand are distributed and candidate sites are selected. Once the data are collected and analysed, identification of planning approaches, deployment options, and formulation of a multiobjective problem follow.

3.2. Planning Approaches. The technical performance and the total cost of a network are a function of the choice of deployment option, architecture selection, choice of technologies, operating bands, and planning and optimization approaches [43, 44].

As far as planning approaches are concerned, one way of minimizing total cost while enhancing network technical performance is upgrading the network where there is data demand. This means upgrading a cell is only a viable option if a current macrocell is unable to satisfy demand. To attain this goal, it is important to characterise both user locations and demand distribution in the service area. This is called the data-driven approach where users and demands are distributed based on realistic data collected from a network management system [11]. Table 2 shows a summary of the planning approaches that are considered in this work.

The planning approaches are briefly described as follows:

(i) *Data-Driven Planning for User Satisfaction and TCO (DDsa).* In this approach, user distribution

Table 1: Summary of related works and gaps.

References	RAT/nature of work	Site selection/demand distribution	Simulation environments	MaMIMO consideration	Optimization/channel estimation
[17, 18]	5G NR/performance analysis of MaMIMO	Arbitrary/not considered	Synthetic environments	Considered	Not applied/theoretical method
[19–23]	5G NR/performance analysis of MaMIMO	Arbitrary/not considered	Realistic environments	Considered	Applied/theoretical and ray tracing
[24]	5G NR/system model cognitive radio networks	Not considered/not considered	Synthetic environments	Not considered	Not applied/theoretical method
[25]	5G NR/capacity optimization	Arbitrary/not considered	Synthetic environments	Considered	Applied/theoretical method
[26–38]	LTE and5G NR/planning of 5G NR networks	Existing sites/not considered	Combination of realistic and synthetic environments	Not considered	Applied/theoretical and ray tracing
[39, 40]	5G NR/optimize 5G base station location	Based on EMF/not demand based	Realistic environments	Considered	Applied/ray tracing
[41]	5G NR/planning of 5G NR networks	Based on EMF/not considered	Realistic environments	Considered	Applied/ray tracing
[11]	5G NR/planning of 5G NR networks	Candidate sites/considered	Realistic environments	Not considered	Applied/ray tracing

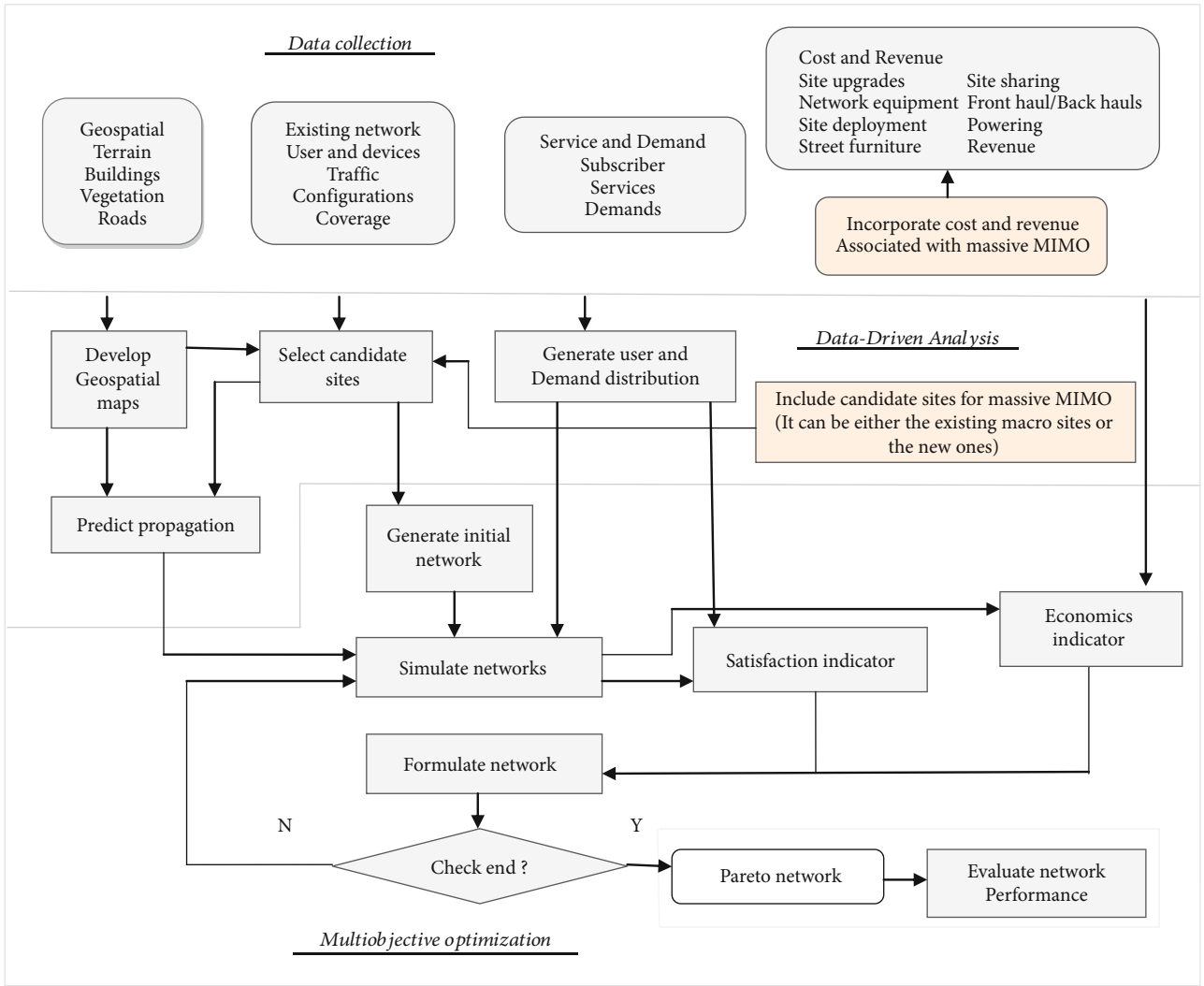

Figure 1: Extended data-driven optimization framework.

Table 2: Planning approaches.

Name	User distribution	Technical objective	Economic objective
Data driven for user satisfaction	Data-driven user distribution	10%-ile user satisfaction	Minimizing total cost
Data driven for aggregate throughput	Data-driven user distribution	Aggregate throughput	Minimizing total cost
Data driven for user throughput	Data-driven user distribution	10%-ile user throughput	Minimizing total cost

and candidate site locations are obtained based on the NMS data from a mobile network operator. The 10%-ile user satisfaction is computed in terms of user throughput, and the total cost is obtained using Equation (1)

(ii) *Data-Driven Planning for Aggregate Throughput and TCO (DDagg)*. This planning approach is similar to DDsa, but it applies aggregate capacity instead of satisfaction

(iii) *Data-Driven Planning for User Throughput and TCO (DDce)*. Again, this planning approach is similar to DDsa, but it applies cell edge throughput instead of satisfaction. Cell edge performance is computed in terms of 10%-ile user throughput

3.3. Deployment Options. As it can be recalled from Subsection 3.2, the deployment option is one of the important parameters associated with both cost and technical performance. As a result, operators must carefully analyse their deployment alternatives based on their business strategy and vendor product plans. Moreover, the options are usually expected to enable a smooth transition to a full 5G network. One way of identifying a cost-effective deployment option is to list every possible option and assess their cost versus

Table 3: Upgrading deployment options.

Configurations	Operating band	Bandwidth
Existing macro (reference configuration)	1800/2600 MHz	40 MHz
Optimized massive MIMO-based 5G NR configuration (DOP1)	3500 MHz	100 MHz
Optimized SC-based 5G NR configuration (DOP2)	3500 MHz	100 MHz
Optimized massive MIMO+SC 5G NR configuration (DOP3)	3500 MHz	100 MHz

technical performance trade-offs. In this work, we consider four deployment alternatives and compared their cost versus performance trade-offs based on the performance target listed in Subsection 3.1. The considered deployment options are

(i) upgrading a network with optimized massive MIMO

(ii) upgrading a network with optimized small cells

(iii) upgrading a network with optimized massive MIMO and small cells

The upgrade options with their configurations are listed in Table 3.

3.4. Multiobjective Problem Formulation. To study a data-driven and multi-objective-based planning approach, a downlink mobile network and small cell candidate locations are considered. The aim is to find an optimal network that provides the best technoeconomic performance among the possible options. To do that, a multiobjective problem is formulated and an evolutionary algorithm is applied as follows.

A 3×1 cellular network having M number of macrosites will have a total of $3M$ macrocells. We assume that the corresponding macrocell locations are considered the candidate site for massive MIMO. Let the notations $X = [X_m, X_s]$, C_m^i and N refer to a network realization, a cell with i and m cell indexes, and number of candidate small cell locations, respectively, where

(i) $X_m = [x_1, x_2, \cdots, x_i, \cdots, x_{3M}]$ represents the macrocell positions and x_i can take a value either 0 or 1. If $x_i = 0$, it refers to the existing cell and $x_i = 1$ refers to massive MIMO

(ii) $X_s = [x_{3M+1}, x_{3M+2}, \cdots, x_{3M+i}, \cdots, x_{3M+N}]$ refers to small cell candidate locations and x_{3M+i} can be either 0 or 1. If x_{3M+i} takes 1, a small cell is deployed in the corresponding site; otherwise, a small cell is not deployed

(iii) the cell index m specifies the serving cell with a value of 1, 2, or 3, representing the macro-, massive MIMO, and small cell, respectively; the notation i denotes that the position of the cell can have a value between 1 and $3M + N$

For a network upgraded with massive MIMO and small cells, the signal-to-interference-plus-noise ratio (SINR) performance of a user located at u per resource block can be expressed as

$$\text{SINR} = \begin{cases} \dfrac{p(u, c_1^z)}{\sum_{i \neq z} p\left(u,\ c_1^i\right) + P_n}, & \text{when a user is associated with macrocell,} \\ \dfrac{p(u, c_2^z)}{\sum_{i \neq z}\left(\sum_{m=2}^{3} p(u, c_m^i)\right) + P_n}, & \text{when a user is associated with massive MIMO,} \\ \dfrac{p(u, c_3^z)}{\sum_{i \neq z}\left(\sum_{m=2}^{3} p(u, c_m^i)\right) + P_n}, & \text{when a user is associated with small cell,} \end{cases} \tag{2}$$

where $p(u, c_1^z), p(u, c_2^z)$, and $p(u, c_3^z)$ are received signal power from macrocell, massive MIMO, and small cell, respectively. The superscript z, $\sum_{i \neq z}(\sum_{m=2}^{3} p(u, c_m^i))$, and P_n are the serving cell index, the sum of interferences from other cells excluding the serving cell, and the noise power. User association is based on reference signal received power (RSRP). Using user SINR, the modulation and coding scheme (MCS) is obtained from the standard SINR to MCS mapping table [45]. Based on these parameters, the corresponding user throughput (TP) can be written as

$$\begin{aligned} \text{TP} = n * N_{\text{RB}} * N_{\text{CPRB}} * \text{mod-sch} * \text{cod-sch} \\ * N_{\text{SYBPSLOT}} * N_{\text{SLOTPSEC}}, \end{aligned} \tag{3}$$

where n is the MIMO layers, N_{RB} is the number of resource blocks, N_{CPRB} is the number of subcarriers per resource

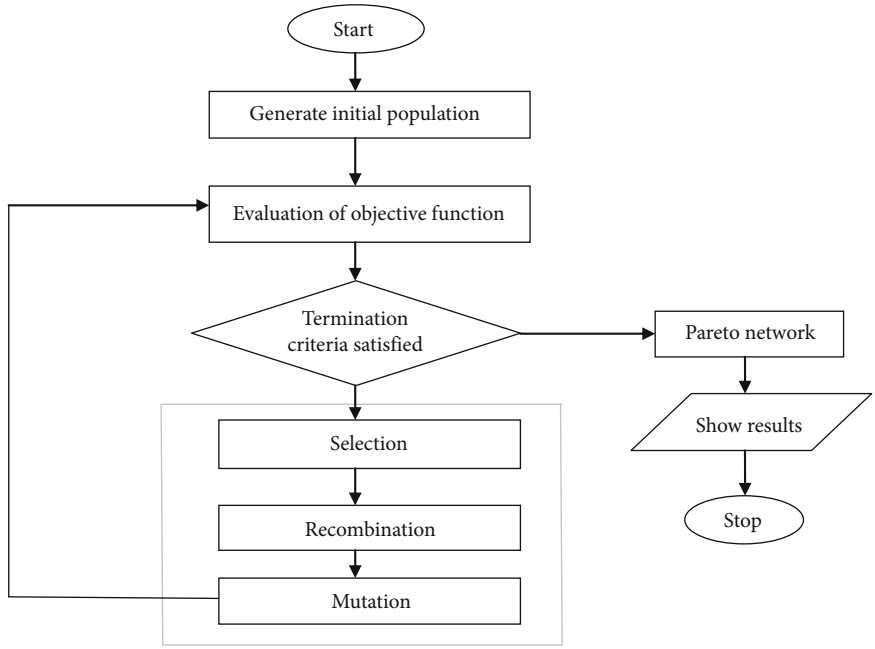

Figure 2: Flow chart of genetic algorithm.

block, mod-sch is the modulation scheme, cod-sch is the coding scheme, N_{SYBPSLOT} is the number of symbols per slot, and N_{SLOTPSEC} is the number of slot per second. Once we get the user throughput, the fitness functions are formulated based on it. Aggregate throughput and user satisfaction are considered technical objectives. If we assume that there are L number of users in the service area and all are served by an existing network, the aggregate user throughput (C_{MB}) can be expressed as

$$C_{MB} = \sum_{n=1}^{L} \text{T}P(u_n). \tag{4}$$

If a network is upgraded with massive MIMO and small cells, traffic is offloaded from macrocells and shared among them. Hence, the aggregate user throughput (C) of the upgraded network can be expressed as

$$C = \sum_{n=1}^{L1} TP(u_n) + \sum_{n=1}^{L2} TP(u_n) + \sum_{n=1}^{L3} TP(u_n), \tag{5}$$

where $\sum_{n=1}^{L1} TP(u_i)$,$\sum_{n=1}^{L2} TP(u_n)$, and $\sum_{n=1}^{L3} TP(u_n)$ are the aggregate user throughput served by macrocell, massive MIMO, and small cell. The notations $L_1, L_2,$ and L_3 are the total number of users served by macrocells, massive MIMO, and small cells, respectively. Based on upgraded and existing aggregate user throughput, network capacity gain (Γ) can be written as

$$\Gamma = \frac{C_{MB} - C}{C_{MB}}. \tag{6}$$

The other objective function is user satisfaction which is a measure of the match between the user demand and networks' ability to full the demand with respect to certain performance indicators like data throughput and latency, which can be defined as [11]

$$S(u, x) = \frac{I(u, x)}{I_d(u)}, \tag{7}$$

where $I(u, x)$ is achieved performance and $I_d(u)$ is demanded performance. In the simulation, the 10%-tile CDF of user satisfaction ($SA_{10\text{per}}$) is used, which can be expressed as

$$SA_{10\text{per}} = S([0.1L]), \tag{8}$$

where S is a vector containing user satisfaction sorted in ascending order. For every R number of macro cells and K number of small cells, there are P numbers of options which can be defined as

$$P = \frac{(3M + N)!}{((3M + N) - (R + K))! * (R + K)!}. \tag{9}$$

From those P options, finding the optimal network presenting the best technoeconomic performance becomes a multiobjective problem. Now, the multiobjective problem is formulated as

$$\text{Min}_x \quad f(x) = [f_1(x), -f_2(x)], \tag{10}$$

where x is a network topology, f_1 is the total cost of the network, and f_2 is the performance of the network that is either aggregate capacity or 10%-tile user satisfaction obtained according to Equations (5) and (8). Multiobjective optimization enables the simultaneous optimization of several objective functions simultaneously. To solve the multiobjective optimization problem in (10), we apply evolutionary algorithms as they are effective metaheuristics for mathematical structures with objective functions without

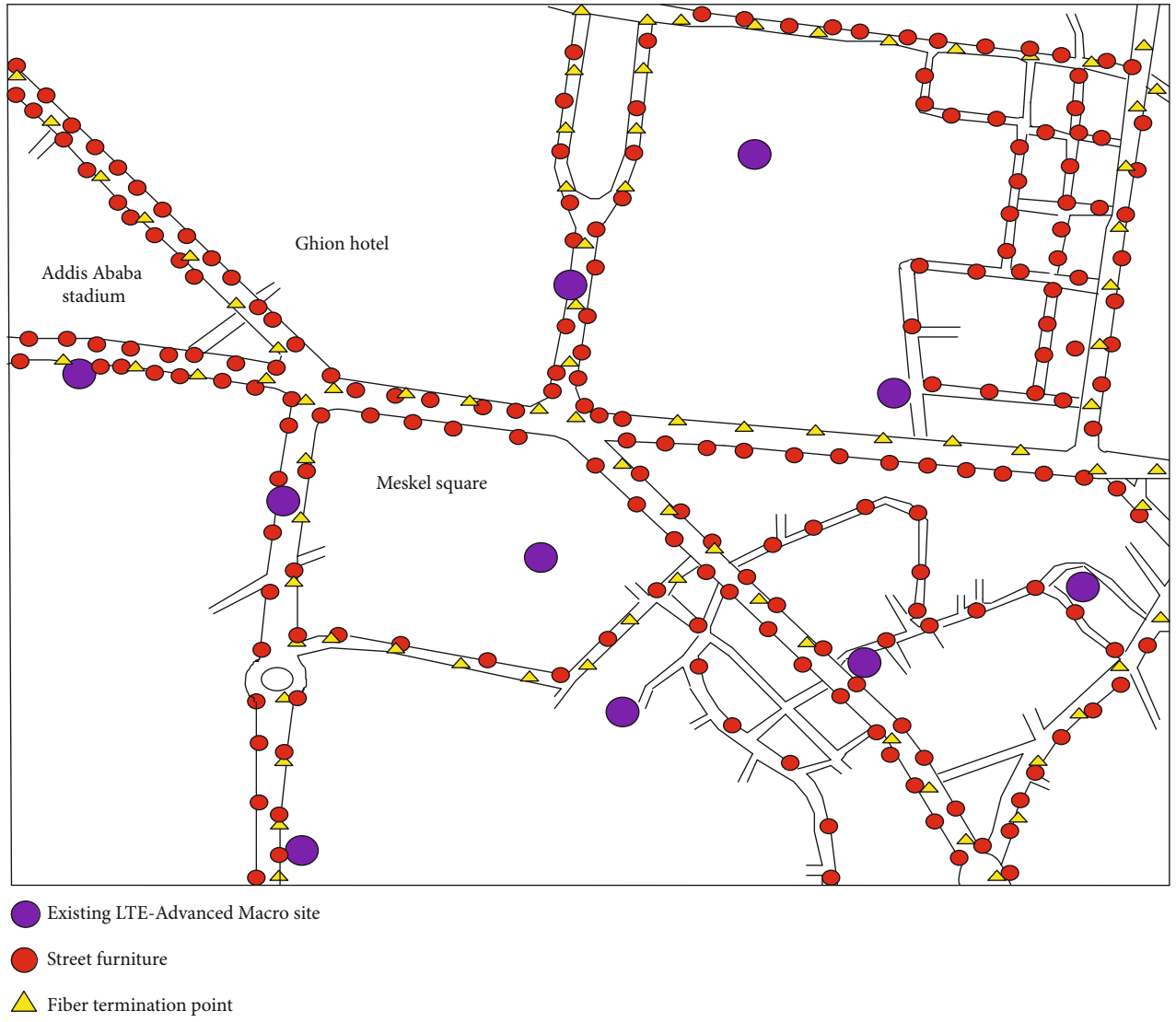

Figure 3: Case study service area around Meskel Square, Addis Ababa.

convexity or continuity [46]. We also select and apply nondominated sorting genetic algorithm II (NSGA-II) due to its less complexity, fast convergence, and empirically near-optimal performance [47] (see Figure 2 for its high-level flow chart).

The NSGA-II algorithm first generates Z number of randomly selected populations which is denoted by the vector V and can be expressed as

$$V = \begin{bmatrix} x_{1,1} & x_{2,1} & \cdots x_{i,1} & \cdots & x_{3M+N,1} \\ \vdots & \vdots & \vdots & \ddots & \vdots \\ x_{1,z} & x_{2,z} & \cdots x_{i,z} & \cdots & x_{M+N,z} \\ & & \vdots & & \\ & & \vdots & & \\ & & \vdots & & \\ & & \vdots & & \\ x_{1,Z} & x_{2,Z} & \cdots x_{i,Z} & \cdots & x_{3M+N,Z} \end{bmatrix}, \quad (11)$$

where $\mathbf{x_{i,z}}$ show the status of macro- and small cells and whether upgrading is applied or not. Each row of vector V consists of randomly selected populations with a different combination of 0 s and 1 s which indicates the status of macrocells and small cell sites. Then, it continues generating evolved populations with better technical and economical performance until the evolution termination criteria are met.

4. Case Study

4.1. Simulation Parameters and Assumptions. In this section, we present a data-driven and multi-objective-based network planning case study with the aim to investigate the performance impact of upgrading a network with massive MIMO or/and small cells for the deployment options and planning approaches that are listed in Tables 2 and 3. The case study is performed for a 4.07 km square (2.81 km × 1.45 km) service area located around Meskel Square, Addis Ababa, Ethiopia (see Figure 3). It is one of the hotspots in Addis Ababa. Currently, the area is being served with an LTE

advanced network with 10 sites (30 macrocells) whose location is depicted with a purple circle in Figure 3.

A 5G new radio uses massive MIMO which is defined by the same synchronisation signal block (SSB) information which contains a primary synchronisation signal, secondary synchronisation signal, and physical broadcasting channel and demodulation reference signal (DM-RS). This work considers a grid of beams-based operations in massive MIMO. That implies the cells broadcast a grid of beams and the user selects the strongest beam based on the strength of reference signal received power (RSRP) and reports the beam index to Next-Generation Node B (gNB). User-centric beams within the same SSB and users within the same beam identification are scheduled with orthogonal resource blocks. Moreover, layers per user are assumed orthogonal.

The NMS follows the number of users attached to different base stations, with the resolution that depends on the cell sizes [11]. The data consists of the cell-level numbers of users and observed per hour data flow with $50\,\text{m} \times 50\,\text{m}$ pixel accuracy based on this data and user density clutter of Table 4, defined by the next-generation mobile network (NGMN) alliance in [48]. The instantaneous user distribution and simulation parameters used in this work are shown in Figure 4 and Table 5, respectively. The performance metrics are computed for various instants of user distribution. The red and small blue spots in Figure 4 show the location of macrosites and the instantaneous location of the users, respectively. User distribution is based on the real data collected from the Ethio Telecom network management system.

For the computation of total costs, we customized the cost analysis presented in [11] as described in Section 3.1. Small cell cost is estimated considering backhaul, site acquisition, site preparation, and small cells and their associated cost as listed in Table 6. On the other hand, the existing macrocells are used as candidates' site locations for massive MIMO. Hence, the cost of massive MIMO is directly proportional to the number of massive MIMO cells assuming no additional location-dependent cost is required, unlike small cells. The total cost of the network is the sum of small cell and massive MIMO costs.

4.2. System-Level Simulation. System-level simulation is carried out using the 5G Vienna system-level simulator with a schematic diagram in Figure 5 after modifying it to fit our network and simulation scenarios. For the simulation, users and demands are distributed based on traffic data collected from Ethio Telecom network management systems. Radio propagation is deterministically computed using Winprop software using terrain and building maps for the service area [49]. The propagation results obtained from Winprop are incorporated into the 5G Vienna simulator for the system-level simulation [45]. The link quality model of the 5G Vienna simulator accepts those parameters as input and provides SINR to the link performance model. Finally, the link performance model takes SINR values and the decision of the scheduler to determine the user throughput as follows. First, the SINR to block error rate (BLER) value is mapped using a 5G standard channel quality indicator (CQI) to the SINR mapping table [45]. Then, based on CQI and the BLER, the numbers of transmitted bits are determined. The throughput performance is used as a fitness value while optimization is performed.

Table 4: User throughput demand and relative density.

Clutter types	Throughput demand (Mbps)	Relative user density
Crowded	1.25	30
Business building	25	15
Residential building	12.5	17.5
Intraurban road (up to 60 km/h)	2.5	4
Others (broadband everywhere)	2.5	1

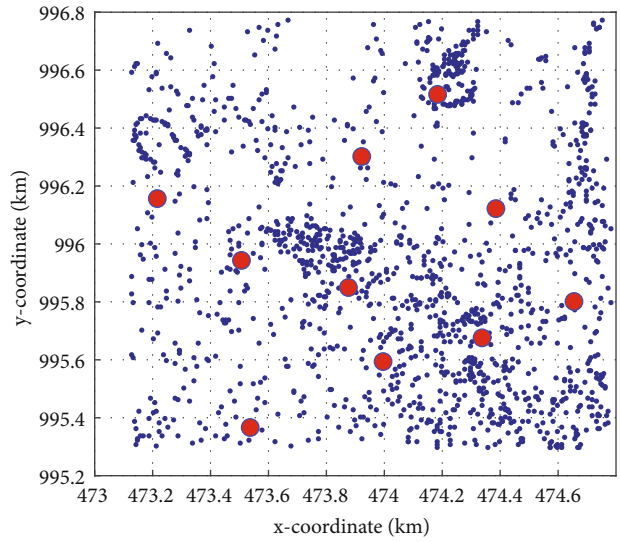

Figure 4: Instantaneous user distribution.

Table 5: Simulation parameters.

Number	Simulation parameters	Values
1	Carrier frequency	3500 MHz
2	Bandwidth	100 MHz
3	Carrier spacing	30 kHz
4	Symbol duration (μs)	33.33 μs
5	Symbols per slot	14
6	Slots per subframe	2
7	Slots per frame	20
8	Layers per cell	4
9	Layers per user	2

4.3. Results and Discussion. User satisfaction, aggregate throughput, and cell edge throughput gain are used as performance metrics to analyse achieved performance results from the system-level simulation. User satisfaction provides a measure for the match between the user demand and networks' ability to realize the demand with respect to certain performance indicators (e.g., throughput) [11]. As stated in

Table 6: Costs relative to 1000 cost unit [11].

	Cost type	Site building	Private building	Street furniture	Other locations
Location dependent	Backhaul civil work	0.025/metre			
	Site acquisition	0.35	0.70	0.35	0.35
	Site rental	0.5	1	0.5	0.25
	Site preparation	0.5	0.5	0.25	1
Location independent	(i) Small cells and their accessories				
	(ii) Small cell installation				
	(iii) Backhauling and electricity				7.19
	(iv) Maintenance and licensing (10% cost of small cell and its accessories)				

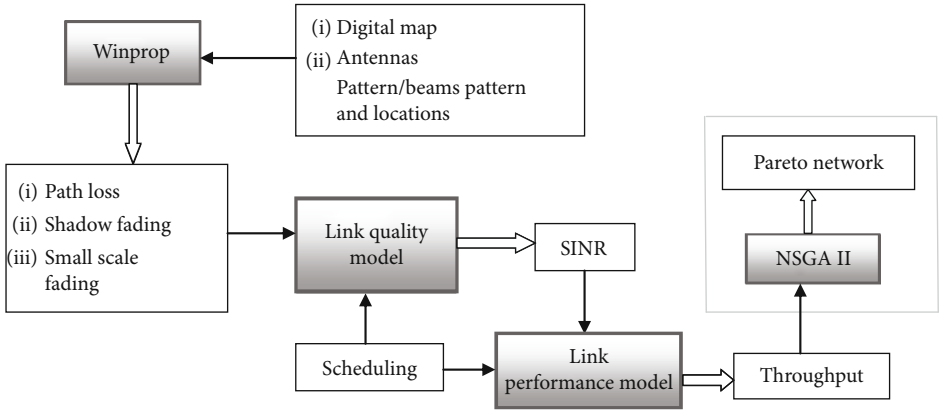

Figure 5: Schematic diagram of system simulation.

Subsection 4.2, the existing macronetwork is taken as a reference (baseline) configuration.

Figure 6 is presented to show the performance impact of the identified planning approaches in terms of a 10%-ile user satisfaction gain assuming a network is upgraded with deployment option DOP1. The planning approaches are DDsa, DDagg, and DDce. As the number of massive MIMO increases, 10%-ile user satisfaction gain also increases for all planning approaches, as shown in the figure. However, since satisfaction is a performance metric, it is natural that the planning approach for DDsa outperforms the other planning options. For example, at the 8 cell Pareto points, the 10%-ile users' satisfaction with DDsa, DDagg, and DDce is about 283.5%, 133%, and 141.5%, respectively. From Figure 6, it can be observed that upgrading a network with deployment option DOP1 and planning approach DDsa provides significant user satisfaction gain compared with a macro-only configuration.

Figure 7 is presented to compare the planning approach DDagg with 5 massive MIMO (DDc5aggmM), DDce with 5 massive MIMO (DDc5cemM), and DDsa with 5 massive MIMO (DDc5samM) in terms of 10%-ile, 50%-ile, and 90%-ile user throughput gains assuming a network is upgraded with deployment option DOP1. The result shows that DDc5cemM outperforms at 10%-ile whereas DDc5aggmM outperforms at 50%-ile and 90%-ile, as can be seen in Figure 7. From Figure 7, it can be deduced that a network that is optimized for one performance target may not provide optimal performance for another performance metric.

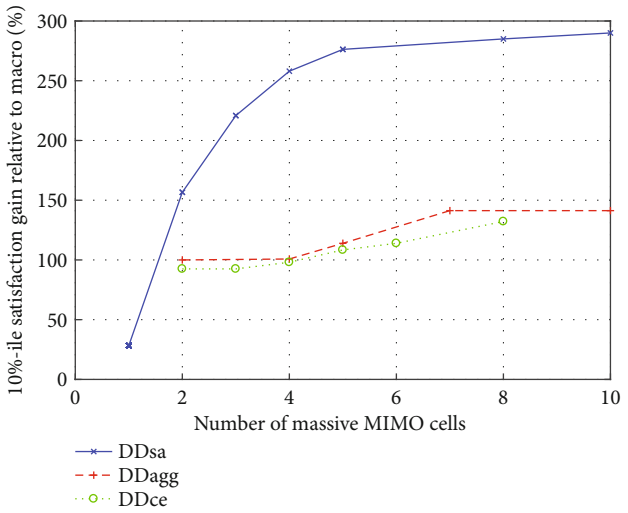

Figure 6: 10%-ile user satisfaction gain relative to macro-only network.

Figure 8 is shown to present the performance impact of planning approach DDagg in terms of aggregate capacity gain assuming a network is upgraded with deployment

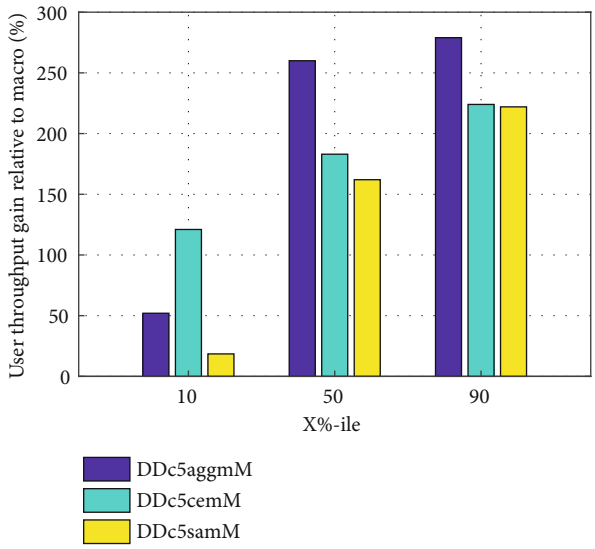

Figure 7: 10%-ile, 50%-ile, and 90%-ile user throughput gain.

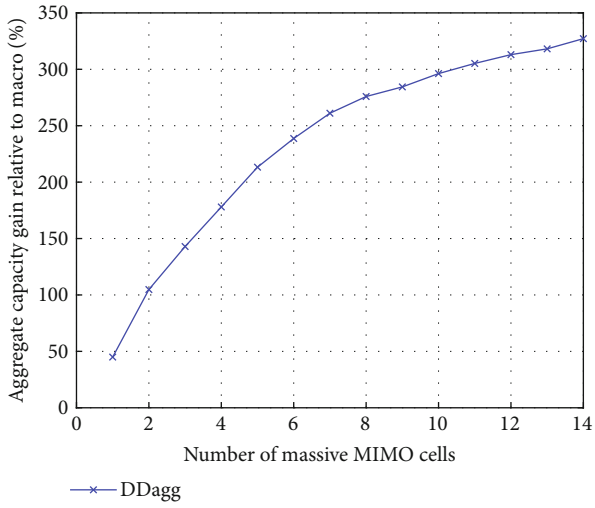

Figure 8: Aggregate capacity gain relative to macro-only network.

option DOP1. The simulation result provides different Pareto points that can optimize a network. As the number of massive MIMO increases, the aggregate capacity gain of planning approach DDagg also increases. For example, at the 12 Pareto massive MIMO planning approach, DDagg provides an aggregate throughput gain of about 311.5%. From Figure 8, it can be noted that upgrading a network with deployment option DOP1 and planning approach DDagg provides considerable aggregate capacity gain relative to a macro-only configuration.

Figure 9 compares the user SINR performance of a network deployed with the planning approach DDagg that has 5 Pareto massive MIMO (ueSINR5cellagmM) and 8 Pareto massive MIMO (ueSINR8cellagmM) to the user SINR performance of macro-only (ueSINR macro only) and massive MIMO-only (ueSINR mMIMO only) networks. Both networks are deployed with deployment option DOP1. As can be seen in Figure 9, both options (ueSINR5cellagmM and ueSINR8cellagmM) significantly improve the SINR performance of the network. From Figure 9, it can be noted that upgrading a network with deployment option DOP1 and planning approach DDagg provides considerable aggregate capacity gain and coverage improvement in terms of SINR relative to a macro-only configuration.

Figure 10 is presented to examine user satisfaction and aggregate capacity gain of upgrading a network with optimized small cells (deployment option DOP2) using planning approaches DDsa and DDagg. The result provides different Pareto points that can enhance user satisfaction and aggregate capacity gain. From Figure 10, it can be noted that upgrading a network with deployment option DOP2 and planning approaches DDsa and DDagg provides considerable user satisfaction and aggregate capacity gain. For example, at 90 Pareto small cell networks, DOP2 with DDsa and DDagg planning approaches provides about 549% user satisfaction gain and 743% aggregate capacity gain over a macro-only configuration.

The normalized cost of different Pareto small cell networks with their corresponding normalized cost for planning option DDagg is indicated in Table 7. The values are normalized with the cost of 182 Pareto networks.

From the above results, it can be noted that a significant performance gain can be obtained from upgrading a network with optimized massive MIMO or optimized small cells. To investigate the aggregate impact of massive MIMO and small cells, two stages and joint optimization are applied. In the case of joint optimization, the Pareto points of small cells and massive MIMO are obtained at the same time. If operators need to optimize their networks jointly, this method is preferable. In the case of two-stage optimization, first, the Pareto points of either of the technologies are identified. Then, the other Pareto points are obtained based on the first Pareto points.

Figure 11 depicts the combined impact of massive MIMO and small cell upgrading on a network with deployment option DOP3 and a two-stage optimization approach. Simulation results provide different Pareto points that can optimize network performance. As the number of small cells increases, user satisfaction gains of small cells without considering massive MIMO (DDsasm), small cells and 5 massive MIMO (DDsasmM5), and small cells and 8 massive MIMO (DDsasmM8) also increase, as shown in Figure 11. Similarly, increasing the number of massive MIMO while keeping the number of massive MIMO user satisfaction also increases. For example, at 50 Pareto networks, the user satisfaction gains of DDsasM, DDsasmM5, and DDsasmM8 are about 379%, 542%, and 664%, respectively. From Figure 11, it can be deduced that upgrading a network with deployment option DOP4 and planning approach DDsa provides a significant user satisfaction gain relative to macro-only configuration. Since DOP3 considers the joint impact of small cells and massive MIMO, it is natural that it outperforms deployment options DOP1 and DOP2, which consider only either massive MIMO or small cells.

Figure 12 shows the user throughput gain performance of deployment option DOP3 applying joint optimization

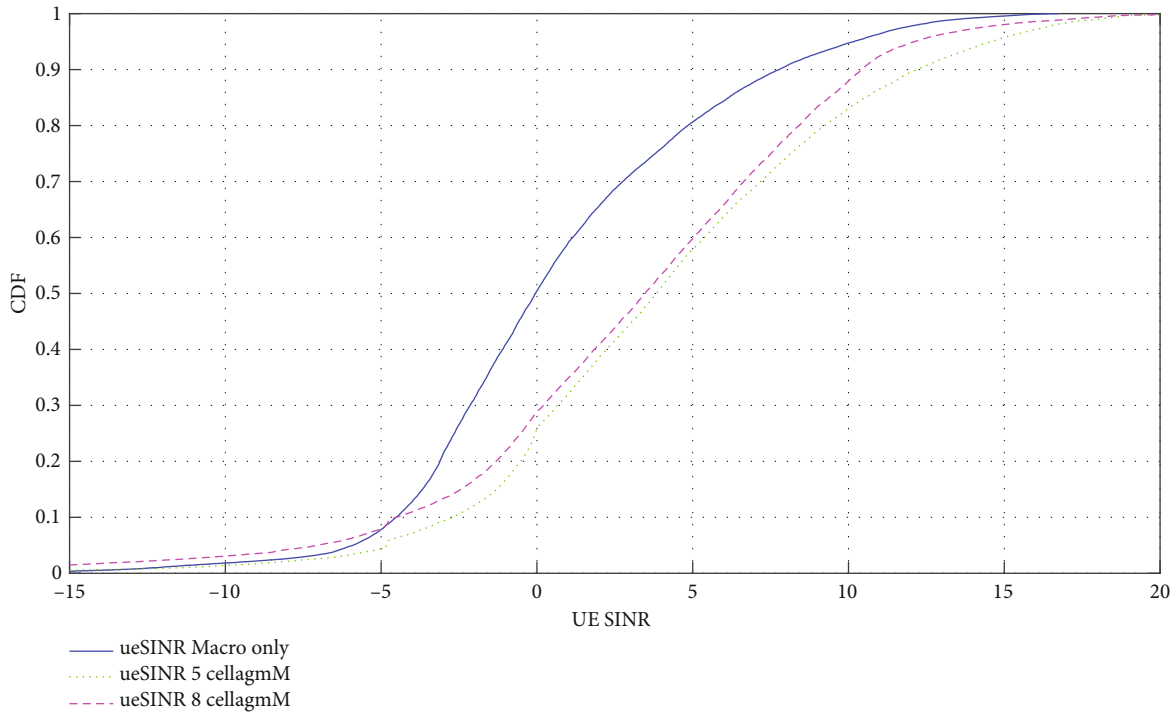

Figure 9: CDF of UE-SINR for macro-only and Pareto networks.

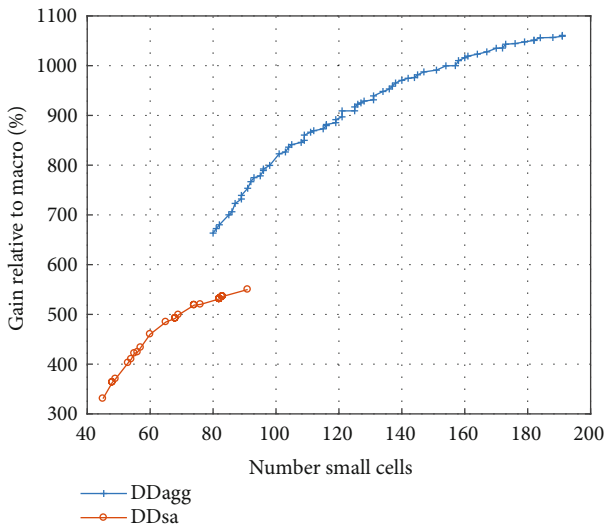

Figure 10: User satisfaction and aggregate capacity gain relative to macro-only network.

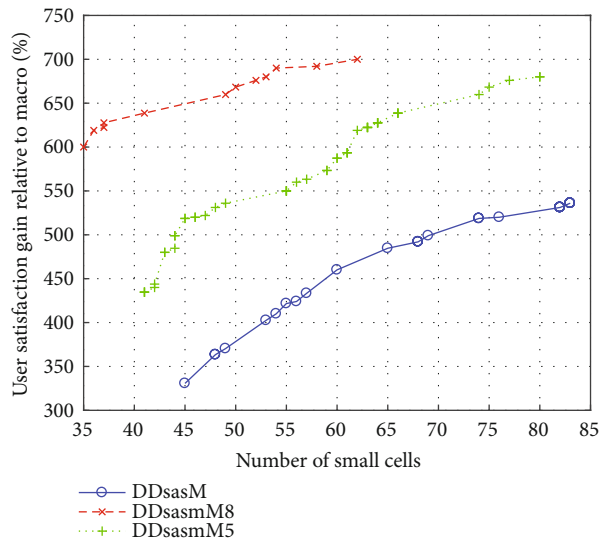

Figure 11: User satisfaction gain with two-stage optimization.

Table 7: Normalized cost of different Pareto small cells.

Pareto small cells	108	116	126	144	172	182
Normalized cost	0.558	0.625	0.681	0.788	0.953	1

with planning approach DDsa. Simulation result provides Pareto points that can enhance user throughput gain. For example, user throughput gain of 5 massive MIMO and 140 small cells (DDsmMc5/140), 1 massive MIMO and 57 small cells (DDsmMc5/140), and 2 massive MIMO and 141 small cells (DDsmMc5/140) at 50%-ile is about 600%, 223%, and 568%, respectively (see Figure 12). From Figure 12, it can be noted that upgrading a network with deployment option DOP3 applying joint optimization with planning approach DDsa improves user throughput relative to the macro-only configuration.

Figure 13 shows the user SINR performance of deployment option DOP3 applying joint optimization with planning approach DDsa. The simulation result provides Pareto points that can enhance user SINR performance. For

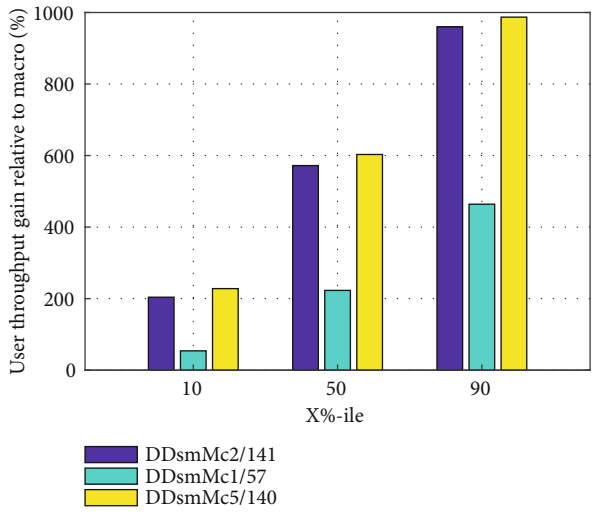

Figure 12: 10%-ile, 50%-ile, and 90%-ile user throughput gain with joint optimization.

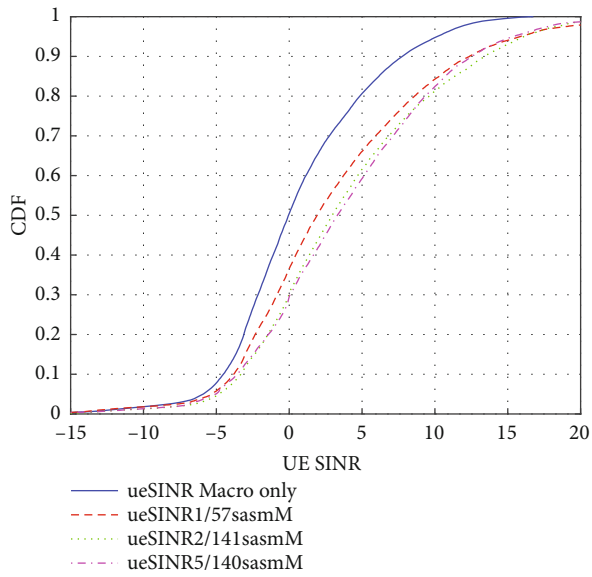

Figure 13: CDF of UE-SINR for macro and Pareto networks with joint optimization.

example, Pareto points with 1 massive MIMO and 57 small cells (ueSINR1/57sasmM), 2 massive MIMO and 141 small cells (ueSINR2/141sasmM), and 5 massive MIMO and 140 small cells (ueSINR5/140sasmM) provide a better SINR performance compared with the macro-only configuration (ueSINR macro only) (see Figure 13). From Figure 13, it can be noted that upgrading a network with deployment option DOP3 applying joint optimization with planning approach DDsa improves SINR performance of a user relative to the macro-only configuration.

Figures 14 and 15 illustrate the aggregate capacity gain of deployment option DOP3 with the planning approach DDagg for joint and two-stage optimization cases. Both options provide Pareto points that can enhance the aggregate capacity of a network. For example, at 100 Pareto points, the aggregate capacity gain of considering only small cells (DDagsM), small cells and 5 massive MIMO (DDaggsmM5), and small cells and 9 massive MIMO (DDaggsmM9) is 818.5%, 1004%, and 1081.5%, respectively (see Figure 15). From Figures 14 and 15, it can be deduced that upgrading a network with deployment option DOP3 and planning approach DDagg provides significant aggregate capacity gain for both joint and two-stage optimization relative to the macro-only configuration. Since DOP3 considers the joint impact of small cells and massive MIMO, it is natural that it outperforms deployment options DOP1 and DOP2.

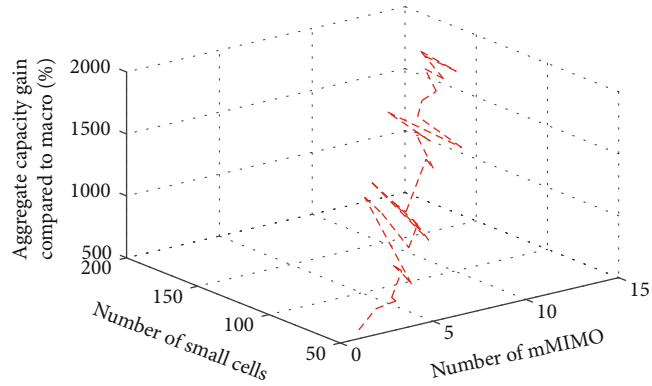

Figure 14: Aggregate capacity gain with joint optimization.

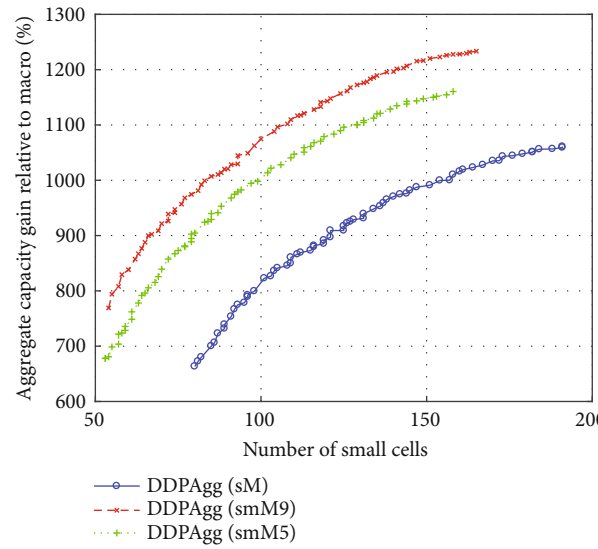

Figure 15: Aggregate capacity gain with two-stage optimization.

Figures 16(a) and 16(b) show user throughput and SINR performance of deployment option DOP3 and planning approach DDagg with two-stage joint optimization. The simulation result gives different Pareto points that can enhance user throughput and SINR performance of a network. For example, user throughput gain of 10 massive MIMO and 117 small cells (DDc10/117smM), 10 massive MIMO and 147 small cells (DDc10/147), and 10 massive

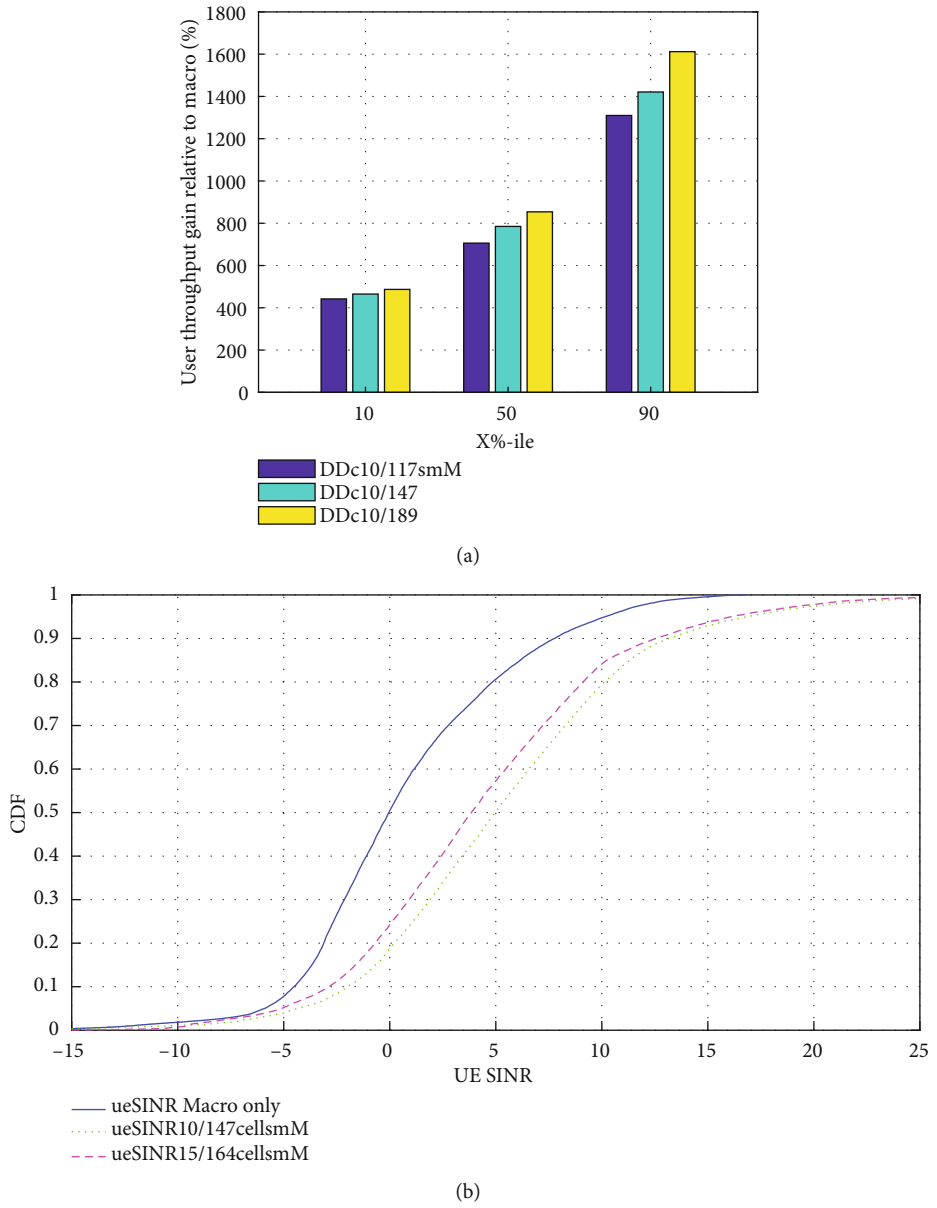

Figure 16: (a) 10%-ile, 50%-ile, and 90%-ile user throughput gain with two-stage optimization. (b) CDF of UE-SINR for macro and Pareto networks with two-stage optimization.

MIMO and 189 small cells (DDc10/189) at 50%-ile is 706%, 785%, and 854%, respectively (see Figure 16(a)). The method also significantly improves the SINR performance of the network at all percentiles compared with the macro-only configuration (see Figure 16(b)). From Figures 16(a) and 16(b), it can be noted that upgrading a network with deployment option DOP3 applying two-stage joint optimization with planning approach DDagg also improves user throughput and coverage capacity relative to the macro-only configuration.

5. Conclusions

In this paper, a data-driven and multiobjective optimization-based 5G RAN planning that utilizes real data from NMS and considers densification with massive MIMO and small cells under a realistic network environment has been investigated. The planning performance has been illustrated using a case study for a selected hotspot area in Addis Ababa. The performance investigation work has included identifying deployment options, planning approach, and multiobjective problem formulation. The simulation campaign has been performed to look for Pareto points for massive MIMO and small cells using a modified planning framework considering the existing LTE-advanced network in the service area. Simulation results showed that the modified planning approach presents network topologies with significant performance gains. For example, upgrading the existing network with optimized massive MIMO will provide up to 311.5% aggregate capacity gain at 12 Pareto locations

relative to the macro-only configuration. For the case of joint two-stage optimization, it provides up to 664% user satisfaction gain for a combination of 8 massive MIMO and 50 small cell Pareto locations. In terms of user throughput, we achieve 706%, 785%, and 854% gain at 50%-ile for 10 massive MIMO common and 117, 147, and 189 respective small cell Pareto locations. Performance impacts of cell-free massive MIMO under realistic simulation environments and extensions of this work for millimetre wave bands are important future work.

Data Availability

The data used to support the findings of this study are available from the corresponding author upon request.

Conflicts of Interest

The authors declare that there are no conflicts of interest regarding the publication of this article.

Acknowledgments

We would like to thank Aalto University for allowing us to use its high-speed computer cluster (Triton) for our computationally intensive simulation campaign. In addition, we would also like to thank Ethio Telecom for the raw network data that is applied for the formulation of user and demand distribution for the case study. We also thank the Institute of Telecommunication TU Wien, Austria, for the Vienna 5G system-level simulator. The Article Processing Charges (APC) of the study will be covered by my coauthors Dr. Edward Mutafungwa and Prof. Jyri Hämäläinen (from Aalto University, Finland).

References

[1] GSMA, "The mobile economy," 2021, https://www.gsma.com/mobileeconomy/wpcontent/uploads/2021/07/GSMA_MobileEconomy2021_3.pdf.

[2] Ericson, "Mobility report," 2021, https://www.ericsson.com/en/reports-and-papers/mobility-report/reports/november-2021.

[3] M. Jaber, Z. Dawy, N. Akl, and E. Yaacoub, "Tutorial on LTE/LTE-a cellular network dimensioning using iterative statistical analysis," *IEEE Communications Surveys & Tutorials*, vol. 18, no. 2, pp. 1355–1383, 2016.

[4] H. Holma and A. Toskala, Eds., *LTE for UMTS: OFDMA and SC-FDMA Based Radio Access*, John Wiley & Sons, 2009.

[5] T. T. Tran, Y. Shin, and O. S. Shin, "Overview of enabling technologies for 3GPP LTE-advanced," *EURASIP Journal on Wireless Communications and Networking*, vol. 2012, no. 1, 12 pages, 2012.

[6] A. Hoglund, D. P. Van, T. Tirronen, O. Liberg, Y. Sui, and E. A. Yavuz, "3GPP release 15 early data transmission," *IEEE Communications Standards Magazine*, vol. 2, no. 2, pp. 90–96, 2018.

[7] D. Astely, E. Dahlman, G. Fodor, S. Parkvall, and J. Sachs, "LTE release 12 and beyond [accepted from open call]," *IEEE Communications Magazine*, vol. 51, no. 7, pp. 154–160, 2013.

[8] M. Kamel, W. Hamouda, and A. Youssef, "Ultra-dense networks: a survey," *IEEE Communications Surveys & Tutorials*, vol. 18, no. 4, pp. 2522–2545, 2016.

[9] D. López-Pérez, M. Ding, H. Claussen, and A. H. Jafari, "Towards 1 Gbps/UE in cellular systems: understanding ultra-dense small cell deployments," *IEEE Communications Surveys & Tutorials*, vol. 17, no. 4, pp. 2078–2101, 2015.

[10] X. Ge, S. Tu, G. Mao, C.-X. Wang, and T. Han, "5G ultra-dense cellular networks," *IEEE Wireless Communications*, vol. 23, no. 1, pp. 72–79, 2016.

[11] B. B. Haile, E. Mutafungwa, and J. Hämäläinen, "A data-driven multiobjective optimization framework for hyperdense 5G network planning," *IEEE Access*, vol. 8, pp. 169423–169443, 2020.

[12] H. Q. Ngo, A. Ashikhmin, H. Yang, E. G. Larsson, and T. L. Marzetta, "Cell-free massive MIMO versus small cells," *IEEE Transactions on Wireless Communications*, vol. 16, no. 3, pp. 1834–1850, 2017.

[13] 5G Americas and Small Cell Forum, "Precision planning for 5G era networks with small cells," 5G Americas and Small Cell Forum, Tech. Rep, 2019.

[14] E. Greenberg and E. Klodzh, "Comparison of deterministic, empirical and physical propagation models in urban environments," in *2015 IEEE International Conference on Microwaves, Communications, Antennas and Electronic Systems (COMCAS)*, pp. 1–5, Tel Aviv, Israel, 2015.

[15] F. Song, J. Li, C. Ma, Y. Zhang, L. Shi, and D. N. K. Jayakody, "Dynamic virtual resource allocation for 5G and beyond network slicing," *IEEE Open Journal of Vehicular Technology*, vol. 1, pp. 215–226, 2020.

[16] E. Björnson, J. Hoydis, and L. Sanguinetti, "Massive MIMO networks: spectral, energy, and hardware efficiency," *Foundations and Trends® in Signal Processing*, vol. 11, no. 3-4, pp. 154–655, 2017.

[17] X. Yu, Y. Hu, G. Gui, S.-H. Leung, W. Xu, and Q. Li, "Performance analysis of uplink massive multiuser SM-MIMO system with imperfect channel state information," *IEEE Transactions on Communications*, vol. 68, no. 10, pp. 6200–6214, 2020.

[18] E. Zeydan, O. Dedeoglu, and Y. Turk, "Experimental evaluations of TDD-based massive MIMO deployment for mobile network operators," *IEEE Access*, vol. 8, pp. 33202–33214, 2020.

[19] X. Gao, O. Edfors, F. Rusek, and F. Tufvesson, "Massive MIMO performance evaluation based on measured propagation data," *IEEE Transactions on Wireless Communications*, vol. 14, no. 7, pp. 3899–3911, 2015.

[20] B. P. Chapa, S. R. Gottapu, and V. K. Mogadala, "Performance analysis of massive MIMO network in downlink scenario," in *2019 International Conference on Wireles Communications Signal Processing and Networking (WiSPNET)*, pp. 252–255, Chennai, India, 2019.

[21] Q. Li, L. Liu, C. Tao, Y. Lu, T. Zhou, and Z. Wei, "Performance analysis of a massive MIMO system in indoor scenario," in *2018 12th international symposium on antennas, propagation and EM theory (ISAPE)*, pp. 1–4, Hangzhou, China, 2018.

[22] M. Aslam, Y. Corre, E. Björnson, and E. G. Larsson, "Performance of a dense urban massive MIMO network from a simulated ray-based channel," *EURASIP Journal on Wireless Communications and Networking*, vol. 2019, no. 1, 2019.

[23] C. Wang, H. Papadopoulos, K. Kitao, and T. Imai, "Ray-tracing based performance evaluation of 5G mmWave massive

MIMO in hotspots," in *2016 International Symposium on Antennas and Propagation (ISAP)*, pp. 608-609, Okinawa, Japan, 2016.

[24] Y. Zeng, H. Yang, Y. Fang, and X. Wang, "Physical layer security for CRNs over Beaulieu-Xie fading channels," *Wireless Communications and Mobile Computing*, vol. 2022, Article ID 6785754, 9 pages, 2022.

[25] J. Ghosh, H. Haci, N. Kumar, K. A. Al-Utaibi, S. M. Sait, and C. So-In, "A novel channel model and optimal power control schemes for mobile mmWave two-tier networks," *IEEE Access*, vol. 10, pp. 54445–54458, 2022.

[26] R. Q. Shaddad, F. S. Al-Kmali, M. A. Noman et al., "Planning of 5G millimeterwave wireless access network for dense urban area," in *2019 First International Conference Of Intelligent Computing And Engineering (ICOICE)*, pp. 1–4, Hadhramout, Yemen, 2019.

[27] C. Tristan and A. Robert, "5G coverage, prediction, and trial measurements," 2020, https://arxiv.org/abs/2003.09574.

[28] R. Q. Shaddad, A. A. Al-Mekhlafi, H. M. Al-Gunid et al., "Densification of 5G wireless access network for urban area at Taiz City, Yemen," in *Recent Trends in Data Science and Soft Computing. IRICT 2018*, vol. 843 of Advances in Intelligent Systems and Computing, , Springer, 2018.

[29] F. Bahlke, O. D. Ramos-Cantor, S. Henneberger, and M. Pesavento, "Optimized cell planning for network slicing in heterogeneous wireless communication networks," *IEEE Communications Letters*, vol. 22, no. 8, pp. 1676–1679, 2018.

[30] Y. Xiao, J. Zhang, and Y. Ji, "Can fine-grained functional split benefit to the converged optical-wireless access networks in 5G and beyond?," *IEEE Transactions on Network and Service Management*, vol. 17, no. 3, pp. 1774–1787, 2020.

[31] P. Muñoz, O. Sallent, and J. Pérez-Romero, "Self-dimensioning and planning of small cell capacity in multitenant 5G networks," *IEEE Transactions on Vehicular Technology*, vol. 67, no. 5, pp. 4552–4564, 2018.

[32] E. J. Oughton, K. Katsaros, F. Entezami, D. Kaleshi, and J. Crowcroft, "An open-source techno-economic assessment framework for 5G deployment," *IEEE Access*, vol. 7, pp. 155930–155940, 2019.

[33] D. Pliatsios, P. Sarigiannidis, I. D. Moscholios, and A. Tsiakalos, "Cost-efficient remote radio head deployment in 5G networks under minimum capacity requirements," in *2019 Panhellenic Conference on Electronics & Telecommunications (PACET)*, pp. 1–4, Volos, Greece, 2019.

[34] A. L. Rezaabad, H. Beyranvand, J. A. Salehi, and M. Maier, "Ultra-dense 5G small cell deployment for fiber and wireless backhaul-aware infrastructures," *IEEE Transactions on Vehicular Technology*, vol. 67, no. 12, pp. 12231–12243, 2018.

[35] C.-W. Tsai, H.-H. Cho, T. K. Shih, J.-S. Pan, and J. J. P. C. Rodrigues, "Metaheuristics for the deployment of 5G," *IEEE Wireless Communications*, vol. 22, no. 6, pp. 40–46, 2015.

[36] C. Ranaweera, E. Wong, A. Nirmalathas, C. Jayasundara, and C. Lim, "5G C-RAN with optical fronthaul: an analysis from a deployment perspective," *Journal of Lightwave Technology*, vol. 36, no. 11, pp. 2059–2068, 2018.

[37] M. Masoudi, S. S. Lisi, and C. Cavdar, "Cost-effective migration toward virtualized C-RAN with scalable fronthaul design," *IEEE Systems Journal*, vol. 14, no. 4, pp. 5100–5110, 2020.

[38] Huawei, "Huawei 5G wireless network planning solution," 2018, https://www-file.huawei.com/-/media/corporate/pdf/white%20paper/2018/5g_wireless_network_planing_solution_en.pdf?la=en-ch.

[39] L. Chiaraviglio, A. S. Cacciapuoti, G. D. Martino et al., "Planning 5G networks under EMF constraints: state of the art and vision," *IEEE Access*, vol. 6, pp. 51021–51037, 2018.

[40] M. Matalatala Tamasala, S. Shikhantsov, M. Deruyck et al., "Combined ray-tracing/FDTD and network planner methods for the design of massive MIMO networks," *IEEE Access*, vol. 8, pp. 206371–206387, 2020.

[41] M. Matalatala, M. Deruyck, E. Tanghe, L. Martens, and W. Joseph, "Optimal low-power design of a multicell multiuser massive MIMO system at 3.7 GHz for 5G wireless networks," *Wireless Communications and Mobile Computing*, vol. 2018, Article ID 9796784, 17 pages, 2018.

[42] D. Jiang, L. Huo, and H. Song, "Rethinking behaviors and activities of base stations in mobile cellular networks based on big data analysis," *IEEE Transactions on Network Science and Engineering*, vol. 7, no. 1, pp. 80–90, 2020.

[43] G. Liu, Y. Huang, Z. Chen, L. Liu, Q. Wang, and N. Li, "5G deployment: standalone vs. non-standalone from the operator perspective," *IEEE Communications Magazine*, vol. 58, no. 11, pp. 83–89, 2020.

[44] M. Agiwal, H. Kwon, S. Park, and H. Jin, "A survey on 4G-5G dual connectivity: road to 5G implementation," *IEEE Access*, vol. 9, pp. 16193–16210, 2021.

[45] M. Muller, F. Ademaj, and T. Dittrich, "Flexible multi-node simulation of cellular mobile communications: the Vienna 5G system level simulator," *EURASIP Journal on Wireless Communications and Networking*, vol. 2018, no. 1, 17 pages, 2018.

[46] Z. Fei, B. Li, S. Yang, C. Xing, H. Chen, and L. Hanzo, "A survey of multi-objective optimization in wireless sensor networks: metrics, algorithms and open problems," *IEEE Communications Surveys & Tutorials*, vol. 19, no. 1, pp. 550–586, 2017.

[47] E. Zitzler and L. Thiele, "Multiobjective evolutionary algorithms: a comparative case study and the strength Pareto approach," *IEEE Transactions on Evolutionary Computation*, vol. 3, no. 4, pp. 257–271, 1999.

[48] NGMN Alliance, "5G white paper," NGMN Alliance, Tech. Rep., 2015.

[49] M. Schoeman, R. Marchand, J. van Tonder et al., "New features in Feko/WinProp 2019," in *2020 International Applied Computational Electromagnetics Society Symposium (ACES)*, pp. 1-2, Monterey, CA, USA, 2020.